European Journal of Pharmaceutics and Biopharmaceutics 72 (2009) 438–443

Contents lists available at ScienceDirect

European Journal of Pharmaceutics and Biopharmaceutics

journal homepage: www.elsevier.com/locate/ejpb

Research paper

Poly(vinyl alcohol) nanoparticle stability in biological media and uptake in respiratory epithelial cell layers *in vitro*

M. Madlova, S.A. Jones *, I. Zwerschke, Y. Ma, R.C. Hider, B. Forbes

Pharmaceutical Science Division, King's College London, London, UK

ARTICLE INFO

Article history:
Received 1 September 2008
Accepted in revised form 16 January 2009
Available online 27 January 2009

Keywords:
Nanoparticle
Airways
Drug delivery
Calu-3
Translocation
Uptake

ABSTRACT

The influence of the size and surface properties of nanoparticles (NP) upon respiratory epithelial cell uptake and translocation is difficult to study, because NP properties are often modified upon suspension in biological fluids. However, a recently developed novel fluorescently labelled poly(vinyl alcohol) (PVA) NP, which does not aggregate in simple biological fluids, is suitable for drug delivery and can be produced with a range of surface properties is a pertinent advance in this field. The aim of this study was to employ the PVA NP to investigate how surface properties influence particle uptake and translocation across Calu-3 epithelial cell layers. Several grades of PVA were synthesised, characterised and labelled covalently with carboxyfluorescein. The labelled PVA was used to fabricate trackable NP that displayed either neutral or positive charge when suspended in Hank's Balanced Salt Solution. The NP were applied to the apical surface of Calu-3 cell layers which internalised up to 11% of the applied particle dose. The maximum fraction that translocated the Calu-3 barrier in 14 h was 1.3%.

1. Introduction

Normal respiration allows single nanoparticles (NP) to deposit in the nasopharyngeal, tracheobronchial and alveolar regions of the airways [1]. However, if particle dispersion, breathing and particle size are controlled, up to 90% of an inhaled NP dose can be specifically deposited in the lower regions of the lung airways [2]. Despite the ability of NP to target distal regions of the lungs, which has the potential to enhanced local or systemic drug delivery, the technical challenge of reproducibly manufacturing and delivering a drug-loaded nanocarrier has prevented commercial exploitation of this technology.

When employed as drug carriers, the large surface area of NP can improve drug dissolution or enhance controlled release compared to micron-sized drug carriers [3]. However, a strong propensity to aggregate [4] the generation of reactive oxygen species [5] and a long-term accumulation in the systemic circulation [6] are potential problems, all of which must be avoided if NP drug carriers are to be used clinically. NP toxicity and aggregation are material specific effects and it can be argued that if the correct material is employed to form the NP, these problems could be avoided. However, the development of a versatile, biocompatible, non-aggregating NP in the dry state is not trivial and the technological challenge of producing such a NP makes the industrial scale development of this material too time consuming and costly for clinical applications.

The aggregation of respirable NP either during storage or during administration produces micron-sized material, which results in the loss of the size-specific advantages of NP and causes problems with aerosolisation and dose heterogeneity. Several strategies have been developed to overcome the problems associated with NP aggregation, including the generation of microencapsulated NP, forced controllable NP aggregation and specific NP surface modification [7], but the nebulisation of an aqueous NP suspension stabilised with a surface active agent remains the simplest and the most effective delivery strategy. Although nebulisers produce micron-sized droplets to deliver NP, once the microparticle deposits upon the airway epithelium, spreading of the liquid phase occurs instantly which results in rapid NP liberation. This strategy has been used to deliver a number of drugs to the lungs, including budesonide [8], insulin [9], rifampacin [10] and itraconazole [11]. However, little is known about the fate of the drug-loaded NP after deposition in the airways of the lungs. For safety and efficacy the drug needs to be released post deposition, followed by effective clearance of the NP. If the NP is retained excessively or is translocated across the epithelium, the potential for local and/or systemic toxicity is raised even when biocompatible materials are employed.

Surprisingly, few studies have been published that report the fate of respirable NP after deposition upon the respiratory epithelium. The data that are available relate to either model NP such as

* Corresponding author. Pharmaceutical Science Division, King's College London, 150 Stamford Street, London SE1 9NH, UK. Tel.: +44 (0)207 848 4843; fax: +44 (0)207 848 48400.
E-mail address: stuart.jones@kcl.ac.uk (S.A. Jones).

0939-6411/$ - see front matter © 2009 Published by Elsevier B.V.
doi:10.1016/j.ejpb.2009.01.009

gold or polystyrene, or those NP that are associated with incidental human exposure such as titanium. Analysis of these reports reveals that, despite using well-defined non-soluble particles that are easier to track compared to those typically employed to administer drugs, there is inconsistency in the nature and extent of NP uptake and translocation reported. Whilst both polystyrene 240 nm NP and gold NP with a size of <100 nm have been shown to translocate the respiratory epithelium [12–15], other reports that show similar-sized NP do not translocate the respiratory epithelium. For example, polystyrene NP with a size range of 20–100 nm translocate rat alveolar cell monolayers [16], whereas radiolabelled carbon NP ranging from 4 to 20 nm in diameter did not pass into the systemic circulation when administered to human subjects [17]. It is notable that many studies are reported with little or no characterisation of the NP in experimental matrices [18–20]. Even physically stable NP suspensions can aggregate on mixing with biological fluids and this may explain, in part, the lack of consistency in the previously published findings [21].

In order to employ NP to deliver drugs to the respiratory epithelium safely, it is necessary to understand the fate of these particles in the lungs. Therefore, the aim of this study was to produce pharmaceutically relevant NP that do not aggregate in cell culture media to investigate the capacity of particles with different physicochemical characteristics to be taken up and translocate across airway epithelial cell layers *in vitro*. Several grades of PVA were produced by altering the percentage hydrolysis of the polymer and these were used to manufacture NP. On the basis of NP charge, size, hydrophobicity and labelling efficiency three grades of PVA were selected for fluorescent labelling to enable the production of NP that could be tracked. Finally, NP formed from the labelled polymers were evaluated for their uptake and translocation in Calu-3 cell layers.

2. Materials and methods

2.1. Materials

Poly(vinyl acetate) (PVAc) (molecular weight (M_w) = 146,000; defined as 'high molecular weight (HMW)' for the purposes of this work), PVAc (M_w = 12,800; defined as 'low molecular weight (LMW)' for the purposes of this work), PVA 80% (M_w = 9000–10,000) and sodium hydroxide pellets were supplied by Sigma–Aldrich (UK). Poly(vinyl pyrrolidone) K_{15} (PVP K_{15}) was supplied from Fluka (Switzerland). Acetone and methanol were sourced from Fisher Scientific (UK). Deuterated solvents deuterium oxide (D_2O) (99.9%) and methanol-d_4 for use in NMR analysis were supplied by Sigma–Aldrich (UK). PVA 40% hydrolysed (M_w = 72,000, defined as 'commercial PVA' for the purposes of this work) was purchased from Polysciences (Eppelheim, Germany). The Calu-3 human bronchial epithelial cell line was purchased from ATCC (MD, USA). Cell culture flasks (162 cm^2 with ventilated caps) and cell culture diffusion systems (0.9 cm^2 polyethylene terephthalate, 1.0 μm pore cell culture supports in 12-well companion plates) were from Becton Dickinson, Labware (NJ, USA), and cell culture-treated sterile 96-well plates were from Costar (through Fisher Scientific, Leicestershire, UK). The 96-well plates for fluorescence studies were from Nunclon Surface (Roskilde, Denmark). Dulbecco's modified Eagle's medium:nutrient mixture F-12 Ham (1:1), minimum essential medium, Hank's Balanced Salt Solution (HBSS), fetal bovine serum (FBS), L-glutamine, penicillin–streptomycin, MEM non-essential amino acid solution, trypsin–EDTA solution (0.25%), trypan blue solution (0.4%), sodium dodecyl sulphate (SDS), and *N*,*N*-dimethyl formamide (DMF) were purchased from Sigma–Aldrich (Poole, UK). The 5(6)-carboxyfluorescein (CF) was from Fluka (Seelze, Germany). Triphenylphosphine, diisopropyl azodicarboxylate and Sephadex® LH-20 were from Sigma–Aldrich (Poole, UK). Fluorescent non-carboxylated polystyrene (PS) NP 0.25 μm was purchased from Duke Scientific (California, USA). *N*-Methyl-2-pyrrolidone was purchased from Sigma–Aldrich (Poole, UK). Ready Protein+™ liquid scintillation cocktail for protein, peptides and nucleic acids was purchased from Beckman Coulter (High Wycombe, UK). [^{14}C]-Mannitol (2.26 GBq $mmol^{-1}$, 61.0 mCi/mM, 3.28 mM final concentration) was purchased from Amersham (Little Chalfont, UK).

2.2. Methods

2.2.1. Poly(vinyl alcohol) synthesis and characterisation

Three different PVA grades (40%, 50% and 60% hydrolysed) were produced using HMW and LMW polymers assuming a stoichiometric 1:1 reaction between the PVAc monomer and the NaOH using a method identical to that published previously [22]. Synthesised PVA samples were prepared for NMR analysis by dissolving 50 mg of each PVA grade in a mixed solvent of methanol-d_4 and deuterated water. The dissolved samples were then centrifuged (DJB Labcare Ltd, Buckinghamshire, England) for 15 min at 13,000 rpm to separate out any residual solid impurities. The supernatant was placed into 5 mm NMR sample tubes, and the samples were analysed at 100 MHz for ^{13}C broadband composite pulse decoupling of protons with a recycle time of 1.35 s and a pulse of 30° for 2 h and 25 min (NMR machine, Bruker, UK). The degree of hydrolysis was calculated as reported previously [22].

2.2.2. Nanoparticle manufacture and characterisation

PVA NP were prepared using a nanoprecipitation method [22]. Briefly, an aqueous dispersing medium consisting of 4 ml of a 10% (w/v) PVA 80% hydrolysed solution, and 26 ml of a 1.54% (w/v) PVP K15 solution, was homogenised for 30 min (L4RT homogenizer, Silverson, East Longmeadow, MA, USA). The diffusing phase (3 ml) containing 1% (w/v) synthesised PVA (labelled with CF) in methanol was added dropwise to the dispersing medium using a syringe pump set at 8 mm/min, from a 5 ml syringe (Razel Scientific Instruments, Inc.). The particle size and zeta potential of the commercial PS and manufactured PVA NP were measured using dynamic light scattering (ZetaPlus®, Brookhaven Instruments Corporation, US) at 25 °C, using a set solid weight concentration of 0.01% (w/v, dilution in HBSS, the medium that was to be employed in the cell culture studies). The stability of the fluorescent probe attached to the polymer was assessed after NP formation by particle suspension in HBSS, followed by ultracentrifugation at 45,000 rpm for 60 min and determination of the free fluorescence at t = 0 and t = 24 h. No significant change in fluorescence was observed over time and the maximum total free fluorescence in all the samples was <0.002% w/w.

2.2.3. Carboxyfluorescein labelling and purification of PVA

A mixture of triphenylphosphine (0.16 mM), PVA (0.0058 mM), diisopropyl azodicarboxylate (0.15 mM) and CF (0.13 mM) in dry DMF (10 ml) was stirred overnight at room temperature [21]. Upon completion of the reaction, the solvent was removed under reduced pressure. The reaction products were re-dissolved in 90:10 methanol/water, and the labelled polymer was separated from the excess CF using a Sephadex LH-20 column with a 90:10 methanol/water elution solvent. The separation was verified and labelling efficiency was calculated according to the methods previously reported by Gul et al. [21].

2.2.4. Fluorescence assay

The PS NP were treated with 75:25 *N*-methyl pyrrolidone:HBSS (pH 8.5) to release and alkalinise the encapsulated fluorescein for reliable quantification in solution. An identical strategy was applied to the PVA-labelled NP in order to maintain a consistent sam-

ple processing method. The NP suspensions (each of which contained different solid weight contents of NP) were diluted in 75:25 *N*-methyl pyrrolidone:HBSS (pH 8.5) to produce the stock solutions of 0. 4 mg/ml. Serial dilutions of the stock solution produced seven calibration standards in the concentration range 0.625–40 μg/ml. Aliquots (100 μl; $n = 6$) of each standard were transferred to a black 96-well plate, and the fluorescence was quantified using a Cytofluor plate reader series 4000 (Perkin-Elmer. Beaconsfield, UK) at an excitation of 485/20 nm, emission of 530/25 nm and a gain of 70. The assay was shown to be fit-for-purpose in terms of intra-day and inter-day reproducibility, i.e. coefficient of variation (CV) <2%.

2.2.5. Culture of Calu-3 cell layers

The Calu-3 human bronchial epithelial cell line was used between passages 32 and 54. Cells were cultured at 37 °C in an atmosphere of 5% CO_2 using a humidified incubator. The cell culture medium was Dulbecco's modified Eagle's medium:nutrient F-12 Ham (1:1) supplemented with 2 mM L-glutamine, 15 mM Hepes, 10% v/v FBS, 1% v/v non-essential amino acid solution and 100 U/ml penicillin and 0.1 mg/ml streptomycin. The cell culture medium was exchanged every 2–3 days, and cells were passaged weekly at a 1:3 split ratio using a 0.25% trypsin–EDTA solution.

Cell layers for the permeability experiments were grown according to the methods of Grainger and co-workers [23]. Briefly, cells were seeded at a density of 10^5 cells/cm^2 on the cell culture supports with 500 μl culture medium in the apical chamber and 1500 μl in the basolateral chamber. After 2 days, the medium was removed from both chambers of the culture system and replaced only in the basolateral chamber of the cell culture support (1500 μl) to provide air interface culture conditions. Cell layers were used for experiments between 9 and 14 days in culture.

2.2.6. Translocation studies

At $t = 0$, 510 μl of the NP suspension was added to the apical surface of confluent Calu-3 cell layers (TER > 300 Ω cm^2, see Table 2 for concentrations in HBSS). Solid weight concentrations of the NP were used to achieve a particle number of 9.77×10^{10} per ml. The conversion of solid weight concentration to particle number was calculated according to the particle manufacturer's instructions:

$$N_p = \frac{6D_f}{\pi P^3\left(D_f + \frac{D_p}{C} - D_p\right)} \quad (1)$$

where N_p is the number of particles, D_f is the density of the fluid, D_p is the density of the particles, P is the particle diameter and C is the particle concentration by mass. Within 1 min, 10 μl of the test solution was removed from the donor solution of each well for analysis to establish the donor concentration (C_o). The translocation experiments were performed at 37 °C using an atmosphere of 5% CO_2 in a humidified incubator under stirring provided by an orbital shaker operated at 50 rpm. At 14 h, the whole donor and receiver fluids were removed, and the amount of NP in these vehicles determined using the fluorescence assay.

The cells were washed by adding HBSS to the apical and basolateral chambers, and the TER of each cell layer was measured as reported previously [24] using chopstick electrodes and an EVOM voltohmmeter (STX-2 and Evom G, World Precision Instruments, Stevenage, UK). The HBSS was removed, and for each NP evaluated ($n = 6$ cell layers), three cell layers were used to assess particle uptake by the cells; thereby enabling an experimental mass balance to be calculated, and three cell layers were used to assess the permeability of a paracellular marker compound; radiolabelled mannitol.

To measure the NP uptake by cells, the donor and receiver chambers were filled with a 10% SDS solution and left overnight to lyse the cells. The next day the SDS solution was collected and the amount of NP in the cell homogenate determined using the fluorescence assay. To measure permeability ($n = 3$ for each NP type), the fluid in the apical chamber was replaced after the measurement of TER by 510 μl of a donor solution containing 8.2×10^{-3} μmol/ml mannitol (specific activity, 2.26 GBq mmol^{-1}) in HBSS and the receiver fluid was replaced by fresh HBSS (1500 μl). Within 1 min, 10 μl of the test solution was removed from the donor solution of each well for analysis to establish the donor mannitol concentration (C_o). The permeability experiments were performed at 37 °C under non-stirring conditions. After 2 h, 10 μl and 500 μl samples were removed from apical and basolateral sides of the cell layer, respectively. Ready Protein™ scintillant (Beckman Coulter, UK), 5 ml, was added to each sample before analysis by liquid scintillation counting using a Multi-Purpose Liquid Scintillation Counter LS 6500 (Beckman Coulter, USA). The appearance of mannitol in the basolateral chamber of the diffusion system was used to calculate the linear transport rate, which was employed to calculate P_{app}:

$$P_{app} = \frac{dQ/dt}{AC_o} \quad (2)$$

where dQ/dt (mol s^{-1}) is the transport rate and indicative of the increase in the amount of mannitol in the receiver chamber per time interval, A (cm^2) is the surface area of the cell culture support, and C_o (mol cm^{-3}) is the initial mannitol concentration in the donor solution.

3. Results and discussion

Partially hydrolysed PVA is a highly versatile co-polymer that has been employed as an excipient in a wide range of pharmaceutical formulations [25]. PVA contains both acetate and alcohol monomer functionalities, and previous work has shown that its amphiphilic nature, conferred by the two monomer subunits that exhibit opposing hydrophobicities, can induce this macromolecule to adsorb at interfaces [26,27]. Using predominantly hydrophobic grades of PVA, NP carriers can be formed in aqueous solvents through simple solvent displacement [22]. Interestingly, the properties of PVA NP have been shown previously to be dependant upon the extent and location of the hydrolysis sites in the polymer chain [22]. Therefore in this study, through control of the reaction conditions, several grades of PVA were synthesised and NP formed prior to selecting which grades of the polymer to label with the CF.

Five PVA batches were synthesised, and the degree of hydrolysis compared to the only hydrophobic grade of PVA that is commercially available (Table 1). Despite the label claim of the commercial material to contain 40% alcohol monomer, it was found to contain only 21% OH groups when analysed by NMR. This confirmed the

Table 1
Nuclear magnetic resonance (NMR) analysis of five poly(vinyl alcohol) (PVA) grades and commercially available PVA. Three diads (OH–OH, OH–Ac and Ac–Ac) occur in the NMR spectra and the ratio of these three peaks was used to calculate the % of alcohol groups (OH). In the description of the grade, the number represents the predicted % hydrolysis, HWM represents high molecular weight and LMW represents low molecular weight. The three grades in bold represent the polymer grades used in the subsequent studies.

Grade	Relative peak area			Hydrolysis (%)
	(OH–OH)	(OH–OAc)	(Ac–Ac)	(OH)
40_{LMW}	**20.75**	**17.92**	**61.32**	**30**
50_{LMW}	27.78	20.37	51.85	38
$40_{commercial}$	**11.30**	**19.13**	**69.57**	**21**
40_{HMW}	**23.33**	**20.83**	**55.83**	**34**
60_{HMW}	56.07	15.89	28.04	64
60_{LMW}	33.90	23.73	42.37	46

Table 2
The physicochemical properties of different % hydrolysis carboxyfluorescein-labelled poly(vinyl alcohol) (PVA) nanoparticles suspended in Hank's Balance Salt Solution at a 0.05 mg/ml. *T* represents time. PS represents polystyrene all measurements that include an estimation of error were preformed three times, and ±1 standard deviation is displayed.

Nanoparticle	Labelling (w/w %)	Size at $T = 0$ (nm)	Size at $T = 24$ (nm)	Charge (mV)
PVA_{30}	0.039	183 ± 11	187 ± 5	13 ± 3
PVA_{34}	0.057	186 ± 2	200 ± 6	19 ± 6
PVA_{21}	0.017	231 ± 9	219 ± 1	3 ± 3
PS	–	293 ± 29	306 ± 19	−13 ± 3

previous findings for this material (Jones, unpublished data). The two grades of PVA synthesised in this study using HMW PVAc generated material which was considered to be close to the target extent of hydrolysis at 34% (predicted 40%) and 64% (predicted 60%), respectively. However, the three grades of PVA produced from LMW PVAc, which should have resulted in 40%, 50% and 60% hydrolysis, produced material that differed considerably from the target extent of hydrolysis at 30%, 38% and 46% hydrolysis, respectively. The reaction between NaOH and PVAc is stoichiometric and the theoretical product specification was based on the equimolar concentrations of reactants, i.e. 1:1, but previous work has shown that the hydrolysis of PVAc is not always complete under these conditions. The greater reaction efficiency when hydrolysing HMW PVAc [22] compared to LMW PVAc [28] was consistent with the previous reports.

The median diameter of the partially hydrolysed PVA NP generated using the solvent displacement technique was dependant upon the % hydrolysis and molecular weight of the polymer employed to form the nanocarrier (Fig. 1). For example, when the partially hydrolysed HMW PVA was used to fabricate the NP, a significant reduction in median diameter of the particles was observed as the % hydrolysis of the polymer increased: 21% (280 nm) > 34% (203 nm) > 64% (177 nm), ($p < 0.05$, ANOVA with post-hoc tukey). The size of the LMW PVA NP was smaller than the HMW material: 30% (168 nm) > 38% (148 nm) > 46% (74 nm). The polydispersity index for all NP manufactured was <0.2; data not shown. The NP size from the nanoprecipitation production method is influenced heavily by the molecular volume that the polymer occupies and by the solubility of the polymer in the final dispersion medium; in this case water. Increasing the proportion of alcohol groups within the polymer has previously been shown to reduce aqueous solubility as a result of an increase in the intramolecular hydrogen bonding [29]. Reducing the solubility of the polymer in the aqueous phase increases the rate of polymer dehydration during the solvent diffusion process, and therefore smaller particles are generated during the NP fabrication process.

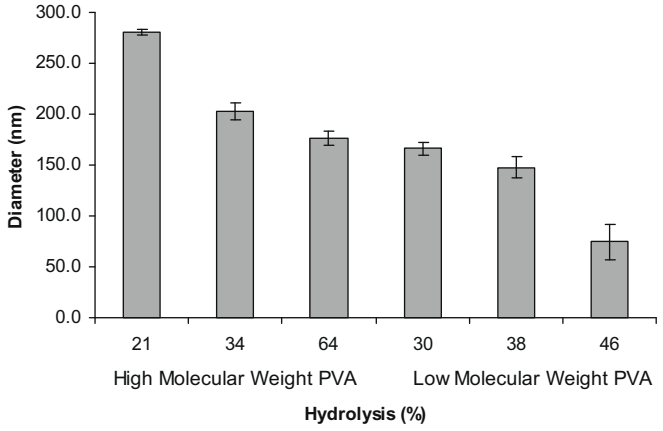

Fig. 1. The influence of poly(vinyl alcohol) (PVA) grade upon the size of the nanoparticles in Hank's Balance Salt Solution. Bars represent the mean ± standard deviation ($n = 10$–30 particle size determinations on up to three batches).

Although it would have been ideal to select a wide range of particle hydrophobicities for the subsequent cell uptake and translocation studies, the CF-labelling efficiency was greatest with the most hydrophobic grades due to the reaction and separation conditions employed [21]. Therefore, the PVA grades selected to generate the CF-labelled NP were PVA HMW 21% hydrolysed (PVA_{21}), PVA LMW 30% hydrolysed (PVA_{30}), and PVA HMW 34% (PVA_{34}). These grades of PVA were chosen as they could be labelled efficiently and they generated NP similar in size whilst still different in terms of hydrophobicity. Of the three selected PVA grades, PVA_{34} and PVA_{30} were labelled most efficiently (Table 2).

In a study designed to investigate fundamentally whether NP penetrate the respiratory epithelium, it is essential that the NP properties are characterised directly in the experimental medium and the properties of the cell barrier are well characterised and reproducible. It has previously been shown that NP with a diameter of 250 nm may not retain their original size when they come into contact with the high salt content and amphiphilic macromolecules found in physiological fluids [21], therefore studies that do not test for NP aggregation can be misleading with respect to understanding how particle properties influence cell uptake and translocation. The lack of characterisation of particles in the experimental media reported in many studies published to date limits their contribution to understanding the fundamental interactions of NP with cells. One of the problems that prevents *in situ* particle size measurement is the inability to assess the particle size of NP in concentrated suspensions using commercially available dynamic light scattering equipment. In this study, the issues caused by a high particle concentration, which can induce multiple/back scattering effects, were addressed by making all *in situ* measurements in a single concentration of 0.01% w/v. Whilst it is accepted that the absolute magnitude of the size and charge may change as a result of particle concentration it was assumed that the comparative trends would remain constant. PVA, an uncharged polymer, displayed a positively charged surface when formed into a NP ranging from +3 to +19 mV (Table 2). In contrast, polystyrene, which contains surface OH functional groups, exhibited a negative charge when the NP were evaluated in HBSS (Table 2). The charge on the PVA particles was assumed to be a consequence of electrolyte adsorption induced by hydration when dispersed in HBSS [30], but like the PS NP it did not lead to any gross particle size changes over the 24 h of suspension in the HBSS (Table 2). There was no statistically significant increase ($p > 0.05$, ANOVA with post-hoc tukey) in the particle size for the PVA_{30} or the PS NP at $t = 0$ compared to that at $t = 24$ h. Furthermore, the PVA_{34} and PVA_{21} NP increased in size by <7% over the 24 h. Although respiratory tract lining fluid *in vivo* has a different composition to HBSS, since the PVA NP display little charge and are physically stable over a wide concentration range (up to 0.05% w/v), it is anticipated that as long as NP are deposited evenly these *in vitro* measurements provide a representation of what will occur in the airways of the lungs.

Unlike NP deposition *in vivo* where multiple clearance mechanisms will operate simultaneously over an extensive surface area that is anatomically difficult to access, using the Calu-3 epithelial cell line that has previously been shown to form tight junctions to provide a representation of airway epithelial barrier with a non-aggregating NP system allows fundamental cell uptake and translocation experiments to be conducted [23]. In the absence of a readily available human cell line that can model the alveolar epithelium *in vitro* [31], the bronchial airway-derived Calu-3 cell line was used, which has been previously employed to assess NP uptake and translocation [24,32]. As the majority of drugs adminis-

tered via inhalation are for local action in the bronchiolar airways, the fate upon the deposition of NP targeted to this region of the lungs (for example, by nebulisation as microdroplets) is of therapeutic relevance. After application of the NP, the Calu-3 cells retained a transepithelial electrical resistance (TER) in the range of 305–609 $\Omega\,cm^2$ and the P_{app} of mannitol was between 2.9 and 5.6×10^{-7} cm/s, which was in accordance with effective *in vitro* epithelial barriers reported previously [32,23]. The permeability and TER of the barrier indicated an absence of any adverse effects as a result of the NP exposure.

Measuring NP translocation provides additional challenges compared to molecules dissolved in solution. The samples taken from the donor and receiver chambers of the diffusion system must be well mixed and physically stable in order to assure a homogeneous sample, the particles must pass largely unhindered through the cell culture support, and dose must be controlled using a suitable metric, e.g. particle number and not mass fraction which is dependant on size. In particular, the pore size of the cell culture support must be such that the epithelial cell layer grows with a suitable degree of cellular differentiation and forms tight intercellular junctions, but must also allow diffusive particle translocation. This means that the commonest type of support, which has 0.4 μm pores, is unsuitable for studying NP translocation [32]. The experimental methodology used in this work was designed to control these potentially confounding issues that arise when studying the kinetics of particulates and allow a direct comparison of NP transport rate in cell layers. In this experiment, the NP were shown to be physically stable (Table 2), three of the four NP (PVA_{30}, PVA_{34}, PVA_{21}) were shown to permeate the cell culture support freely, all the NP suspensions applied to the cells were equivalent in terms of particle number (9.77×10^{10} per ml), mass balance was determined by removal of the whole liquid volume, and a robust and sensitive assay (developed in the previous work; Ref. [21]) was used to quantify the NP concentration.

The NP assessed in the uptake and translocation studies were of similar size, i.e. 200–300 nm, but the particles were made from materials that displayed different physicochemical properties. In terms of hydrophobicity, the NP were theoretically ranked as PVA_{34} < PVA_{30} < PVA_{21} < PS according to the properties of the materials from which they were fabricated. The most hydrophilic particles in this set displayed the most extensive transport through the blank cell culture support at 63 ± 11% (PVA_{30}) and 64 ± 6% (PVA_{34}). In addition, these particles gave the highest recovery for the cell line translocation experiment at 93% and 91% for the PVA_{30} and the PVA_{34} NP, respectively. The PS NP did not pass the cell culture support and <40% of the PVA_{21} NP crossed the support. As the PS NP were unable to traverse the cell culture supports, the translocation of these NP through the cells could not be measured. The differences in the NP transport through the cell culture support suggest that the study of NP translocation across the blank membrane should always be performed irrespective of whether the NP are similar in size and do not aggregate in the dispersion medium.

The PVA NP were internalised most extensively at ca. 11% (Fig. 2). The uptake of PVA NP by the Calu-3 cell line was independent of surface charge or particle hydrophobicity, but it was significantly higher ($p < 0.05$, *t*-test) compared to the negatively charged PS NP (7 ± 1%). The measurement of uptake may have included particles adsorbed to cell surfaces, but the excellent physical stability of all the particles in the application vehicle, HBSS, demonstrates a favourable NP-vehicle interaction, making this solvent efficient at removing adsorbed particles during the washing stages of the translocation study protocol. In addition, confocal images confirmed qualitatively that particles were internalised within the cells (data not shown).

To date, few studies have been published that investigate the mechanism by which airway epithelial cells internalise particles

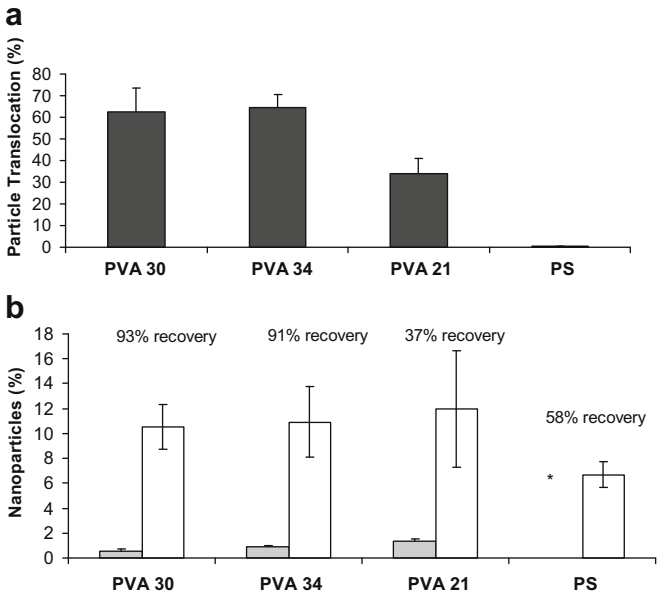

Fig. 2. Nanoparticle (NP) translcoation through blank cell culture supports (a) and particle uptake (white) and translocation (grey) across Calu-3 cell layers (b). * indicates that NP translocation was not measurable as the particles did not pass through the blank culture support. In the description of the NP, the number represents the % hydrolysis, PVA represents poly(vinyl alcohol) PS represents polystyrene 250 nm NP.

even though a number of studies have reported particulate entry to the body via this route of exposure [12,14]. A number of different particle uptake mechanisms have been distinguished for eukaryotic cells including phagocytosis, macropinocytosis, clathrin—mediated endocytosis and non-clathrin—mediated endocytosis (which includes internalisation via caveolae). The mechanism of particle uptake is dependant upon the properties of the particles. For example, Rejman et al. [33] showed that particles <200 nm were predominantly internalised via clathrin coated pits, whilst particles with a diameter >200 nm were internalised via caveolae-mediated endocytosis in a murine melanoma cell. In the present study, although no attempt was made to assess the cell uptake mechanism, the data were consistent with the work of Rejman et al. [33] who suggested that caveolae-mediated endocytosis of particles >200 nm is driven by preferential membrane–particle electrostatic interaction, which favours positively charged particles. Caveolae are thought to be present in the cell membrane of the Calu-3 epithelial cells [34], and it is possible that a non-specific, charge driven caveolae internalisation process is responsible for particle uptake in these cells.

Translocation of PVA NP through the cells was much less extensive compared to the cell uptake of NP. The most hydrophobic particle, PVA_{21}, which possessed little surface charge, demonstrated the most extensive translocation at 1.3 ± 0.3% of the particle dose whereas 0.9 ± 0.1% and 0.5 ± 0.2% of the applied PVA_{34} and PVA_{30} NP crossed the cells. The relatively low % of NP that passed through the cells suggested that once sequestered the NP are retained inside the cell and do not translocate readily.

4. Conclusions

Given the concerns over the potential for adverse effects of NP in the vasculature [35], understanding how and why NP are transported across airway epithelial cells is critical in order to be able to assess the toxicological impact of new materials and to facilitate the rational design of effective inhaled NP drug carriers [36]. The data presented in this study illustrate that in order to discover

how the properties of NP influence cell uptake, characterisation of the particles must be performed in the cell lining fluid as the particles can acquire a different charge and display a different particle size compared to their original specification. NP with a diameter of up to 300 nm were found to be internalised by Calu-3 cells. However, only low levels of NP translocation were observed suggesting that NP will have the opportunity to release their drug pay load prior to cell translocation, enabling effective delivery to the airway epithelium to be achieved.

References

[1] G. Oberdorster, E. Oberdorster, J. Oberdorster, Nanotoxicology: an emerging discipline evolving from studies of ultrafine particles, Environ. Health Perspect. 113 (2005) 823–839.

[2] J. Heyder, J. Gebhart, G. Rudolf, C.F. Shiller, Deposition of particles in the human respiratory tract in the size range 0.005–15 μm, J. Aerosol. Sci. 17 (1986) 811–825.

[3] D.F. Emerich, C.G. Thanos, Targeted nanoparticle-based drug delivery and diagnosis, J. Drug Target 15 (2007) 163–183.

[4] C. Vauthier, B. Cabane, B.D. Labarre, How to concentrate nanoparticles and avoid aggregation?, Eur J. Pharm. Biopharm. 69 (2008) 466–475.

[5] S. Rodoslav, L. Laibain, A. Eisenberg, M. Duisica, Micellar nanocontainers distribute to defined cytoplasmic organelles, Science 300 (2003) 615–618.

[6] D.V. Bazile, C. Ropert, P. Huve, T. Verrecchia, M. Marlard, A. Frydman, M. Veillard, G. Spenlehauer, Body distribution of fully biodegradable [^{14}C]-poly(lactic acid) nanoparticles coated with albumin after parenteral administration to rats, Biomaterials 13 (1992) 1093–1102.

[7] P.G.A. Rogueda, D. Traini, The nanoscale in pulmonary delivery. Part 2: Formulation platforms, Exp. Opin. 4 (2007) 607–620.

[8] W.K. Kraft, B. Steiger, D. Beussink, J.N. Quiring, N. Fitzgerald, H.E. Greenberg, S.A. Waldman, The pharmacokinetics of nebulised nanocrystal budesonide suspension in healthy volunteers, J. Clin. Pharm. 44 (2004) 67–72.

[9] Y. Kawashima, H. Yamamoto, H. Takeuchi, S. Fuioka, T. Hinto, Pulmonary delivery of insulin with nebulised DL-lactide/glycolide copolymer (PLGA) nanospheres to prolong hypoglycaemic effect, J. Control. Release 62 (1999) 279–287.

[10] R. Pandy, G.K. Khuller, Antitubercular inhaled therapy: opportunities, progress and challenges, J. Antimicrob. Chemother. 55 (2005) 430–435.

[11] J.T. McConville, K.A. Overhoff, P. Sinswat, Delivery of nebulised itraconazole nanoparticles in the murine model, in: R.N. Dalby, R.P. Byron, J. Peart, J.D. Sunman (Eds.), Respiratory Drug Delivery Europe, vol. 1, Davis Healthcare International Publishing, Illionois, 2005, pp. 281–283.

[12] T. Kato, T. Yashiro, Y. Murata, D.C. Herber, K. Oshikawa, M. Bando, S. Ohno, Y. Sugiyama, Evidence that exogenous substances can be phagocytised by alveolar epithelial cells and transported into blood capillaries, Cell Tissue Res. 311 (2003) 47–51.

[13] T. Bajanowski, B. Brinkmann, A.M. Stefanec, R.H. Barckhaus, G. Fechner, Detection and analysis of tracers in experimental drowning, Int. J. Legal Med. 111 (1998) 57–61.

[14] W.G. Kreyling, M. Semmler, F. Erbe, P. Mayer, S. Takenaka, H. Schultz, Translocation of ultrafine insoluble iridium particles from the lung epithelium to extrapulmonary organs is size dependant but very low, J. Toxicol. Environ. Health A 65 (2002) 1513–1530.

[15] M.F. König, J.M. Lucocq, E.R. Weibel, Demonstration of pulmonary vascular perfusion by electron and light microscopy, J. Appl. Physiol. 75 (1993) 1877–1883.

[16] N.R. Yacobi, L. Demaio, J. Xie, S.F. Hamm-Alvarez, K.J. Kim, E.D. Crandell, Polystyrene nanoparticles trafficking across alveolar epithelium, Nanomedicine 4 (2008) 139–145.

[17] N.L. Mills, N. Amin, S.D. Robinson, A. Anand, J. Davies, D. Patel, J.M. de la Fuente, F.R. Cassee, N.A. Boon, W. MacNee, A.M. Millar, K. Donaldson, D.E. Newby, Do inhaled carbon nanoparticles translocate directly into the circulation of humans?, Am J. Respir. Crit. Care Med. 173 (2006) 426–431.

[18] M.A. Videira, M.F. Botelho, A.C. Santos, L.F. Gouveia, J.J.P. De Lima, A.J. Almedia, Lymphatic uptake of pulmonary delivered radiolabelled solid lipid nanoparticles, J. Drug Target 10 (2002) 607–613.

[19] A. Nemmar, P.H.M. Hoet, B. Vanquickenborne, D. Dinsdale, M. Thomeer, M.F. Hoylaerts, H. Vanbilloen, L. Mortelmans, B. Nemery, Passage of inhaled particles into the blood circulation in humans, Circulation 105 (2002) 411–414.

[20] J.P. Berry, B. Arnoux, G. Stanislas, P. Galle, J. Chrtien, Microanalytic study of particle transport across alveoli—role of blood platelets, Biomed. Express 27 (1977) 354–357.

[21] M. Gul, S.A. Jones, L.A. Dailey, Y. Maa, A. Aramanb, F. Sadouki, R. Hider, B. Forbes, A poly(vinyl alcohol) nanoparticle platform for kinetic studies of inhaled particles, Inhaled Toxic., in press.

[22] J. Chana, B. Forbes, S.A. Jones, The synthesis of high molecular weight partially hydrolysed poly(vinyl alcohol) grades suitable for nanoparticle generation, J. Nanosci. Nanotechnol. 8 (2008) 5739–5747.

[23] C. Grainger, L.L. Greenwell, D.J. Lockley, G.P. Martin, B. Forbes, Culture of Calu-3 cells at the air–liquid interface provides a representative model of the airway epithelial barrier, Pharm. Res. 23 (2006) 1482–1490.

[24] A. Grenha, C.I. Grainger, L.A. Daily, B. Seijo, G.P. Martin, C. Remunan-Lopez, B. Forbes, Chitosan nanoparticles are compatible with respiratory epithelial cells in vitro, Eur. J. Pharm. Sci. 31 (2007) 73–84.

[25] S.A. Jones, M.B. Brown, G.P. Martin, Determination of polyvinyl alcohol using gel filtration liquid chromatography, Chromatographia 59 (2004) 43–46.

[26] S.A. Jones, G.P. Martin, M.B. Brown, Manipulation of beclomethasone–hydrofluoroalkane interactions using biocompatible macromolecules, J. Pharm. Sci. 95 (2006) 160–1073.

[27] F. Buttini, P. Colombo, M. Wenger, P. Mesquida, C. Marriott, S.A. Jones, Back to basics: the development of a simple, homogenous, two-component dry powder inhaler formulation for the delivery of budesonide using miscible vinyl polymers, J. Pharm. Sci. 97 (2008) 1257–1267.

[28] S.A. Jones, S. Mesgarpour, J. Chana, B. Forbes, Preparation and characterisation of polymeric nanoparticles using low molecular weight poly(vinyl alcohol), J. Biomed. Nanotechnol. 4 (2008) 319–325.

[29] W.S. Lyoo, H.W. Lee, Synthesis of high-molecular-weight poly(vinyl alcohol) with high yield by novel one-batch suspension polymerization of vinyl acetate and saponification, Colloid Polym. Sci. 280 (2002) 835–840.

[30] R.M. Pashley, Hydration forces between mica surfaces in aqueous electrolyte solutions, J. Colloid Interface Sci. 83 (1981) 531–546.

[31] J.L. Sporty, L. Horalkova, C. Ehrhardt, In vitro cell culture models for the assessment of pulmonary drug disposition, Exp. Opin. Drug Metab. Toxicol. 4 (2008) 333–345.

[32] J. Geys, L. Coenegrachts, J. Vercammen, Y. Engelborghs, A. Nemmar, B. Nemery, P.H.M. Hoet, *In vitro* study of the pulmonary translocation of NPs: a preliminary study, Toxicol. Lett. 160 (2006) 218–226.

[33] J. Rejman, V. Oberle, I.S. Zuhorn, D. Hoekstra, Size dependent internalisation of particles via the pathways of clathrin and caveolae mediated endocytosis, J. Biochem. 377 (2004) 159–169.

[34] N.A. Bradbury, J.A. Clark, S.C. Watkins, C.C. Widnell, H.S. Smith, R. Bridges, Characterization of the internalization pathways for the cystic fibrosis transmembrane conductance regulator, Am. J. Physiol.: Lung Cell. Mol. Physiol. 276 (1999) L659–L668.

[35] A. Radomski, P. Jurasz, D. Alonso-Escolano, M. Drews, M. Morandi, T. Malinski, M.W. Radomski, Nanoparticle-induced platelet aggregation and vascular thrombosis, Br. J. Pharmacol. 146 (2005) 882–893.

[36] C. Medina, M.J. Santos-Martinez, A. Radomski, O.I. Corrigan, M.W. Radomski, Nanoparticles: pharmacological and toxicological significance, Br. J. Pharmacol. 150 (2007) 552–558.